Chalcogenide Letters Vol. 19, No. 4, April 2022, p. 241 - 257

Effect of substrate temperature on some optical properties of SnO:ZnS_4, SnO:CoS_4 SnO:CuS_4 and SnO:Cr^{3+} thin films deposited using spray pyrolysis technique

C. A. Elekwa[a], C. N. Ukwu[b,*], P. E. Agbo[a,c], O. C. Ozibo[a]
[a]*Ebonyi State University Abakaliki*
[b]*AlexEkwueme Federal University Ndufu Alike, P.M.B. 1010, Abakaliki, Ebonyi State*
[c]*King David University of Medical Sciences, Uburu, Nigeria*

Tin oxide (SnO) thin films is one of the most extremely studied oxides because of its usefulness in UV-detector. SnO is known for wide bandgap of 3.6eV which makes it a good candidate for window layers in heterjunction solar cells. Transition metal chalcogenides (TMCs) exhibits unique properties such as high conversion efficiency, good absorption coefficient and good bandgap energy which make their thin films versatile as a coating materials. Spray pyrolysis have been used to deposit SnO (core), SnO/ZnS, SnO/CrS, SnO/CoS and SnO/CuS (biphasic) at 0.1M concentration and different substrate temperatures of 100^{o}C, 150^{o}C and 200^{o}C. The effect of varying substrate temperatures on the optical and structural properties of the SnO (core) and SnO/TMCs (biphasic) films were examined and analysed. The result showed that the optical transmittance decreased with increase in substrate temperature for SnO (core). The result showed that the absorbance of the SnO thin films at various substrate temperatures vary from 0.10 – 0.7. For the biphasic films, SnO/ZnS, SnO/CrS, SnO/CoS and SnO/CuS the absorbance decreases in the neighbourhood of 300nm-350nm, increases from 350nm-600nm and decreases between 600-100nm for the different substrate temperature of 100^{o}C, 150^{o}C and 200^{o}C. The reflectance spectra of SnO films were found fluctuating between maxima and minima while biphasic films altered the reflectance which showed very low reflectance as observed. The bandgap energy for SnO are 2.00eV, 2.10eV, and 2.20eV at 100^{o}C, 150^{o}C and 200^{o}C substrate temperature. The energy band gap increased with substrate temperature. Whereas for biphasic films, the bandgap was in the neighourhood of 1.10eV-1.60eV for the different substrate temperature. The extinction coefficient (k) of SnO films increased with increase in substrate temperature while in biphasic films, the extinction coefficient showed significant reduction in magnitude irrespective of the substrate temperature. The refractive index of all the film samples were generally low irrespective of the substrate temperature. The films:SnO and biphasic displayed low value of dielectric constant irrespective of the substrate temperature. The result equally reveals that the optical conductivity for SnO decreases with increase in the substrate temperature.

(Received November 25, 2021; Accepted April 5, 2022)

Keywords: Substrate temperature, Optical properties, Biphasic films and spray pyrolysis, Transistion metals

1. Introduction

As one of the most extremely studies, the usefulness of tin oxide (SnO) thin films in UV detector is known for its wide band of 3.6eV. This makes it a good candidate for window layers in heterjunction solar cells. Transition metal chalcogebides (TMCs); Zinc (II) sulphide (ZnS), chromium (ii) sulphide (CrS), cobolt (ii) sulphide (CoS) and copper (ii) sulphide (CuS) are refractory compounds. These films exhibit unique properties such as high conversion efficiency, good absorption coefficient, good bandgaps and corrosion resistance. These properties make their films versatile as coating materials. Cadium Sulphide (Cds) thin films which are widely used as window layers in CIGS are toxic. Therefore, an alternative window layers are currently being

* Corresponding author: ukwunweke@yahoo.com
https://doi.org/10.15251/CL.2022.194.241

researched to replace CdS. Thus, SnO and biphasic composites are potential materials for possible incorporation in CIGS solar cells.

2. Methodology

Deposition of biphasic nanostructured composite materials of the form SnO/TMCs enables us to produce thin films which combined with the unique properties of transition elements and that of oxide of tin. This chemical combination is for wider range of applications using spray pyrolysis technique. The solutions were prepared using analytical grade reagents. Biphasic composites (SnO/TMCs) were deposited on the substrate using spray pyrolsis. The data obtained from the characterization were analysed to ascertain their Structural, optical and solid state properties for possible device applications.

3. Results

3.1.Transmittance

Figures 1-5 are plots of transmittance Vs wavelength for SnO, SnO/ZnS, SnO/CoS, SnO/CrS, SnO/CuS deposited at substrate temperature of 100 ^{0}C, 150 ^{0}C and 200 ^{0}C.

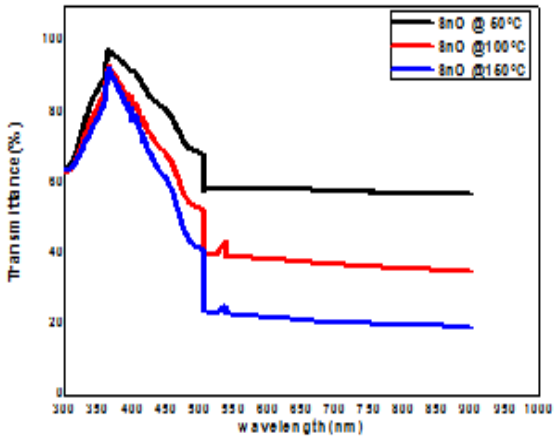

Fig. 1. Transmittance Vs Wavelength for SnO @ 100 ^{0}C, 150 ^{0}C, and 200 ^{0}C.

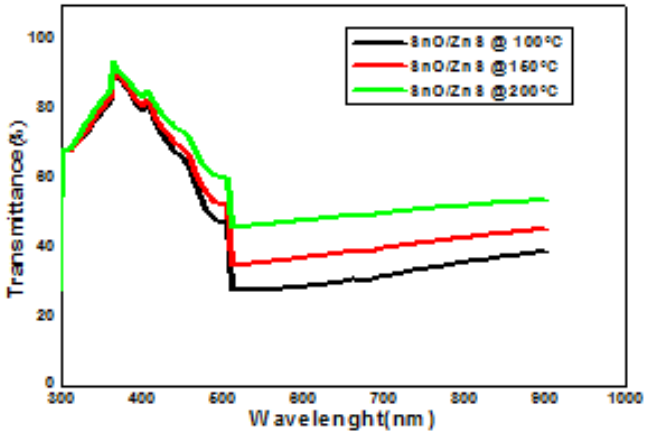

Fig. 2. Transmittance Vs Wavelength for SnO/ZnS @ 100^{O}C, 150^{O}C & 200^{o}C.

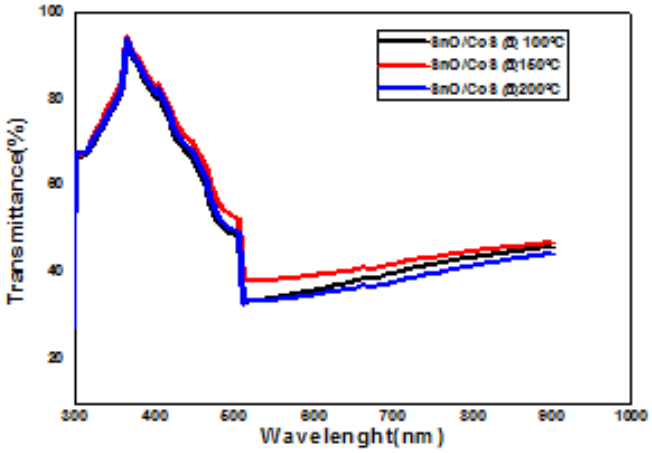

Fig. 3. Transmittance Vs Wavelength for SnO/CoS @ 100^{O}C, 150^{O}C & 200^{o}C.

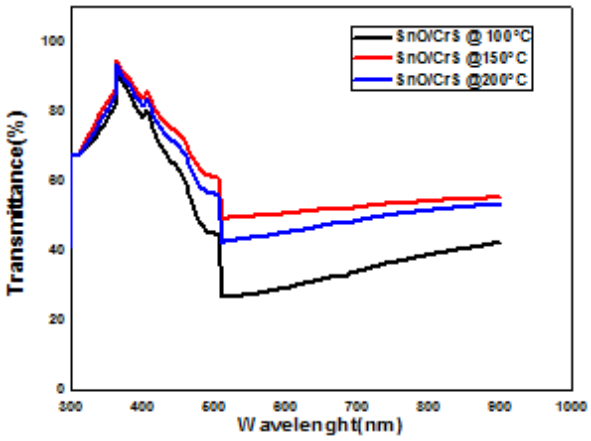

Fig. 4. Transmittance Vs Wavelength for SnO/CrS @ 100^{O}C, 150^{O}C & 200^{o}C.

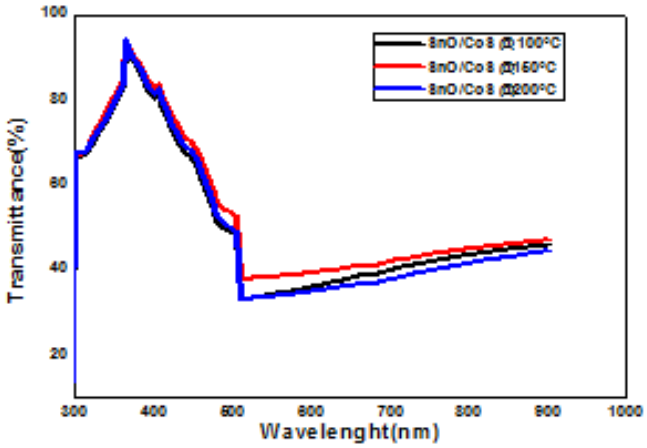

Fig. 5. Transmittance Vs Wavelength for SnO/CuS @ 100^{O}C, 150^{O}C & 200^{o}C.

3.2.Absorbance

Figures 6-10 are plots of Absorbance Vs Wavelength for SnO, SnO/ZnS, SnO/CoS, SnO/CrS, SnO/CuS deposited at substrate temperature of 100^{o}C, 150^{o}C and 200^{o}C.

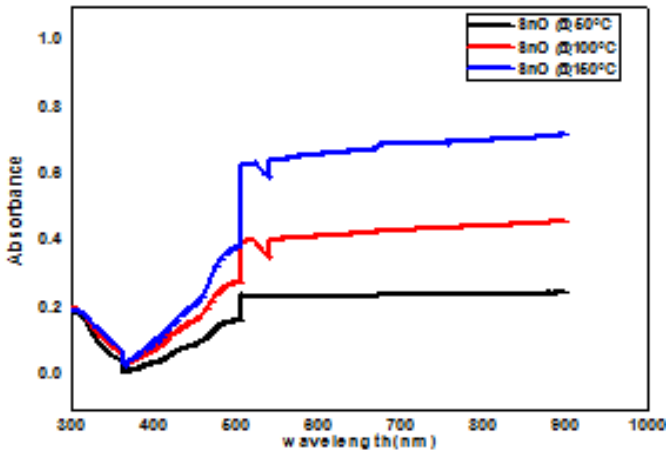

Fig. 6. Absorbance Vs Wavelength for SnO @ 50^o 100^o 150^o.

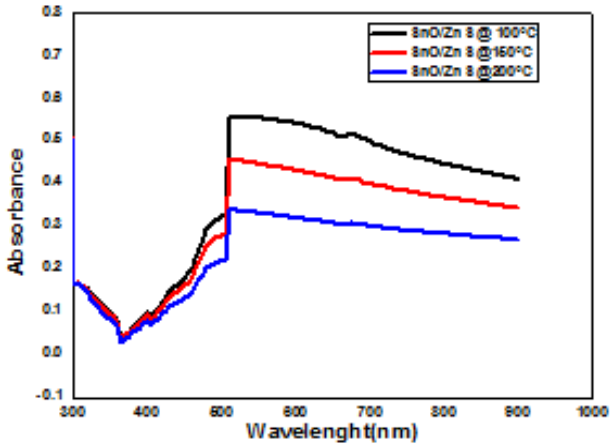

Fig. 7. Absorbance Vs Wavelength for SnO/ZnS @ 100^{O}C, 150^{O}C & 200^{o}C.

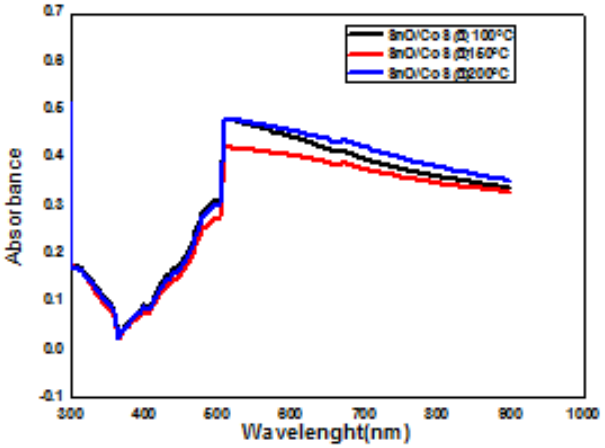

Fig. 8. Absorbance Vs Wavelength forSnO/CoS@ 100^{O}C, 150^{O}C & 200^{o}C.

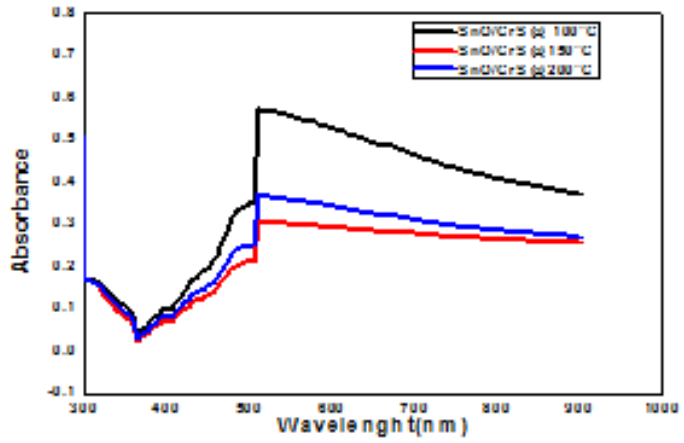

Fig. 9. Absorbance Vs Wavelength for SnO/CrS @ 100^{O}C, 150^{O}C & 200^{o}C.

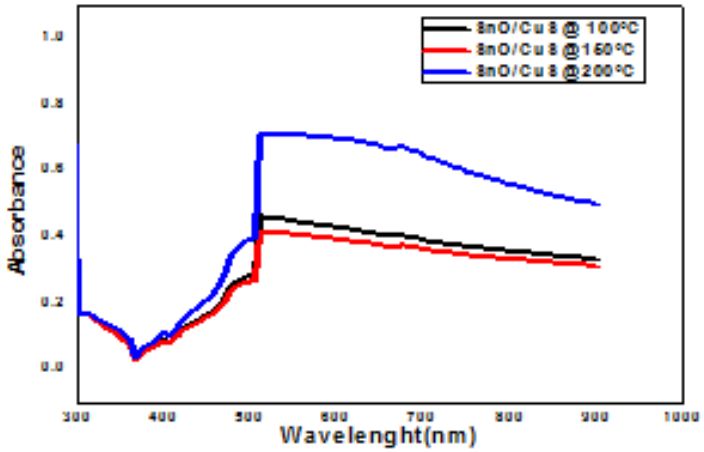

Fig. 10. Absorbance Vs Wavelength for SnO/CuS @ 100^{O}C, 150^{O}C & 200^{o}C.

3.3.Reflectance

Figures 11-15 are plots of Reflectance Vs Wavelength for SnO, SnO/ZnS, SnO/CoS, SnO/CrS, SnO/CuS deposited at substrate temperature of 50^{o}C, 100oC, 150^{o}C and 200^{o}C.

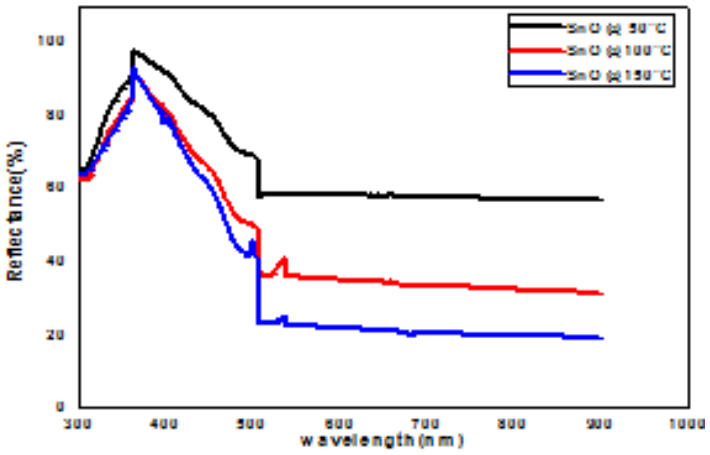

Fig.11. Reflectance Vs Wavelength for SnO @ 100 ^{0}C, 150 ^{0}C and 200 ^{0}C.

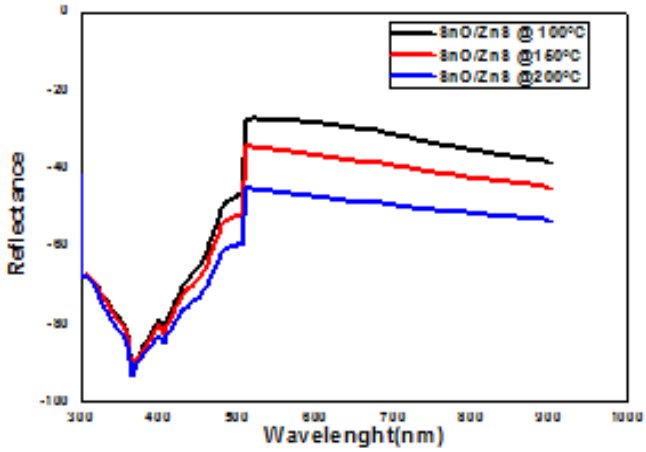

Fig. 12. Reflectance Vs Wavelength for SnO/ZnS @ 100^{O}C, 150^{O}C & 200^{o}C.

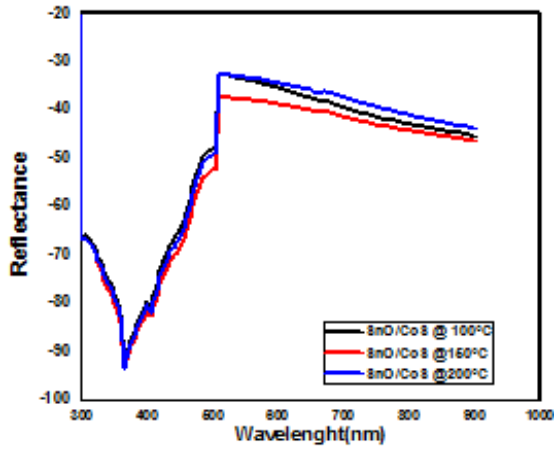

Fig. 13. Reflectance Vs Wavelength for SnO/CoS @ 100^{O}C, 150^{O}C & 200^{o}C.

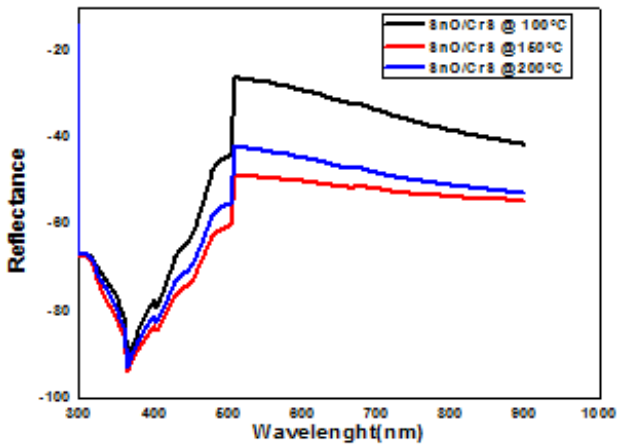

Fig. 14. Reflectance Vs Wavelength for SnO/CrS @ 100^{O}C, 150^{O}C & 200^{o}C.

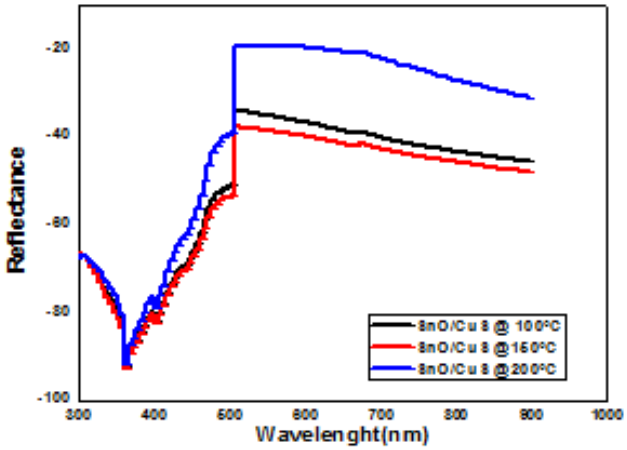

Fig. 15. Reflectance Vs Wavelength for SnO/CuS @ 100^{O}C, 150^{O}C & 200^{o}C.

3.4.Refractive Index

Figures 16-20 are plots of Refractive Index Vs hv (eV) for SnO, SnO/ZnS, SnO/CoS, SnO/CrS, SnO/CuS deposited at substrate temperature of 50^{o}C, 100oC, 150^{o}C and 200^{o}C.

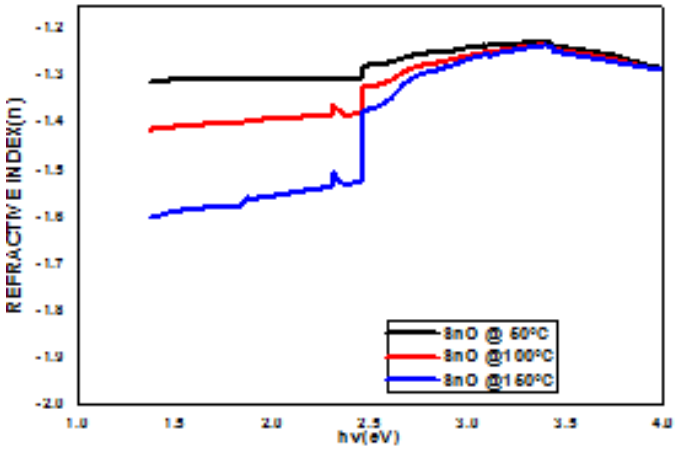

Fig. 16. Refractive Index Vs h v (e V) for SnO @ 100 ^{o}C, 150 ^{o}C and 200 ^{o}C.

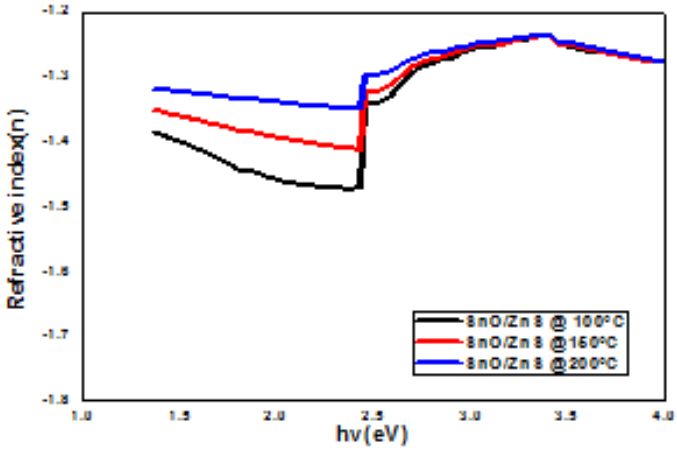

Fig.17. Refractive index (n) Vs hv(eV) for SnO/ZnS @ 100^{O}C, 150^{O}C and 200^{o}C.

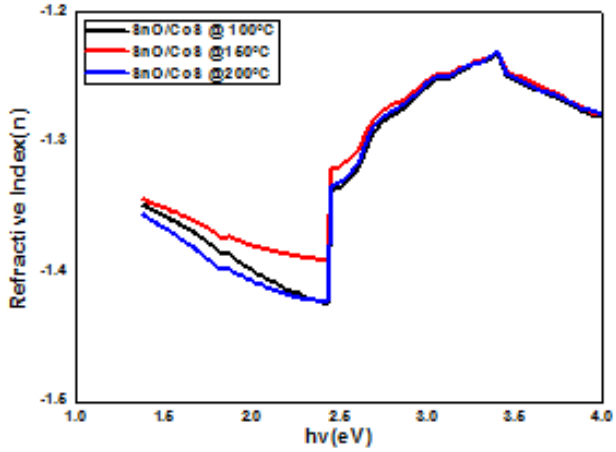

Fig. 18. Refractive index (n) Vs hv(eV) for SnO/CoS @ 100^{O}C, 150^{O}C and 200^{o}C.

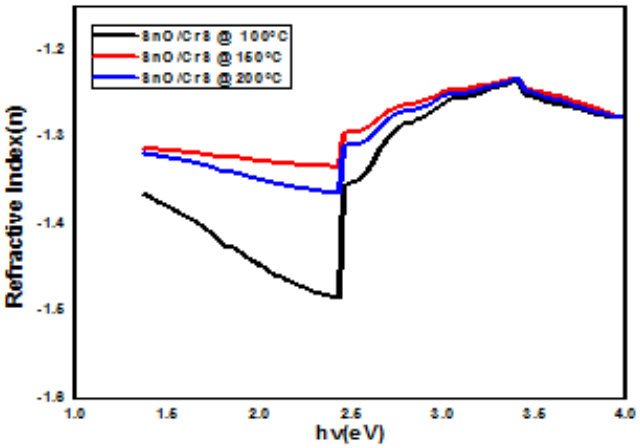

Fig. 19. Refractive index (n) Vs hv(eV) for SnO/CrS @ 100^{O}C, 150^{O}C & 200^{o}C.

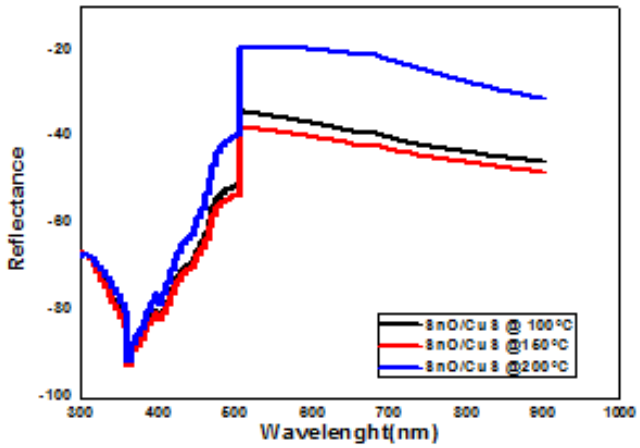

Fig. 20. Refractive index (n) Vs hv(eV) for SnO/CuS @ 100^{O}C, 150^{O}C & 200^{o}C.

3.5 Extinction coefficient

Figures 21-25 are plots of Extinction coefficient Vs hv (eV) for SnO, SnO/ZnS, SnO/CoS, SnO/CrS, SnO/CuS deposited at substrate temperature of 50^{o}C, 100^{o}C, 150^{o}C and 200^{o}C.

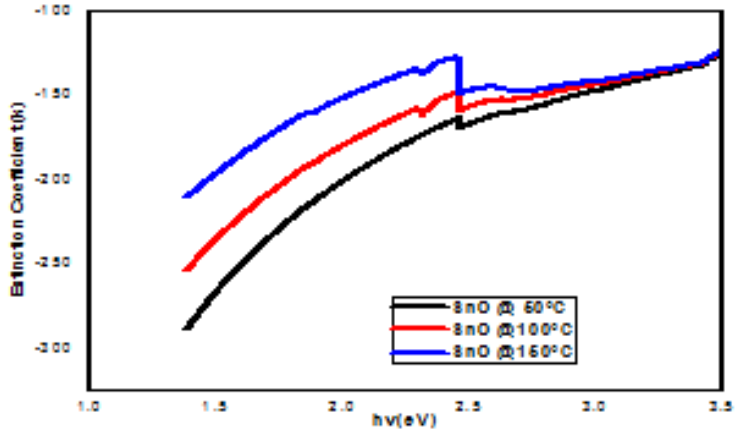

Fig.21. Extinction Coefficient Vs hv(eV) for SnO 100,150 and 200 ^{o}C.

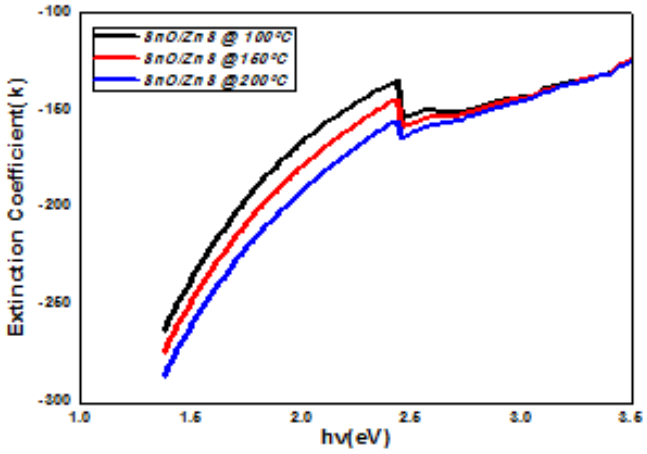

Fig. 22. Extinction Coefft Vs hv(eV) for SnO/ZnS @ 100^{O}C, 150^{O}C & 200^{o}C.

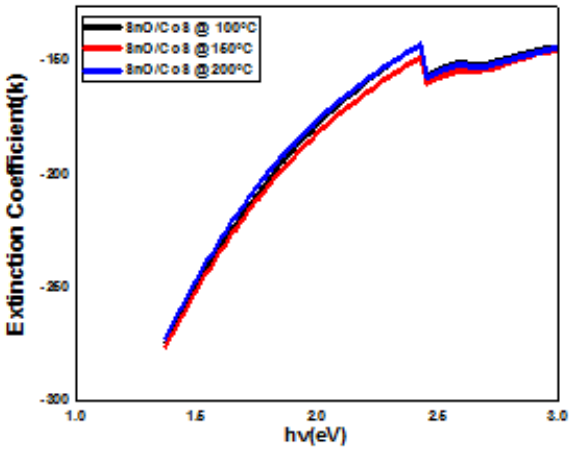

Fig. 23. Extinction Coefft Vs hv(eV) for SnO/CoS @ 100^{O}C, 150^{O}C & 200^{o}C.

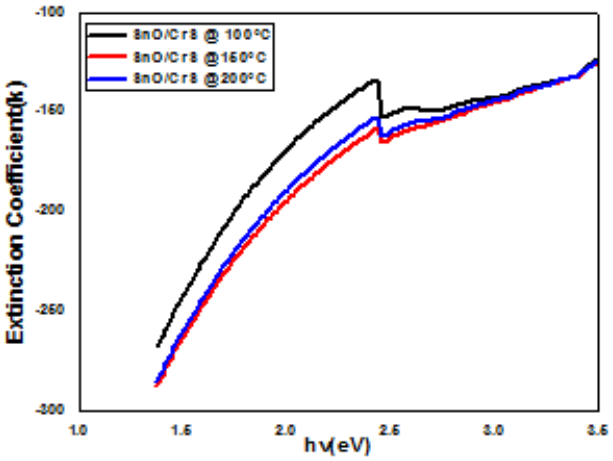

Fig. 24. Extinction Coeff. Vs hv(eV) for SnO/CrS @ 100^{O}C, 150^{O}C & 200^{o}C.

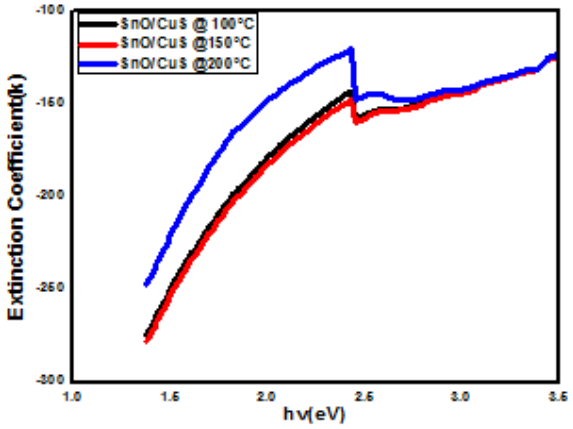

Fig. 25. Extinction Coeff. Vs hv(eV) for SnO/CuS @ 100^{O}C, 150^{O}C & 200^{o}C.

3.6. Band gap energy

Figures 26-30 are plots of $(\alpha hv)^2$ (eV^2m^{-2}) Vs hv(eV) for determination of Band gap Energy for SnO, SnO/ZnS, SnO/CoS, SnO/CrS, SnO/CuS deposited at substrate temperature of100^{o}C, 150^{o}C and 200^{o}C.

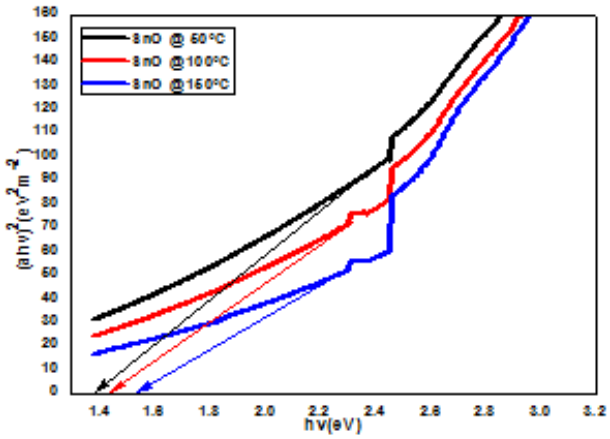

Fig. 26. $(\alpha hv)^2$ (eV^2m^{-2}) Vs hv(eV) for SnO for 50^{o} 100^{o} 150^{o}.

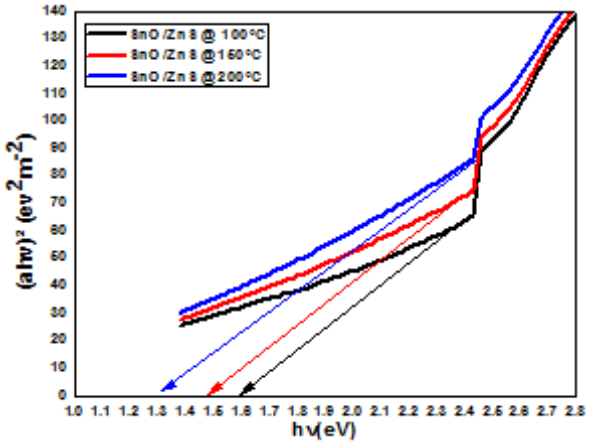

Fig. 27. $(\alpha hv)^2$ (eV^2m^{-2}) Vs hv(eV) for SnO/ZnS @ 100^OC, 150^OC & 200^oC.

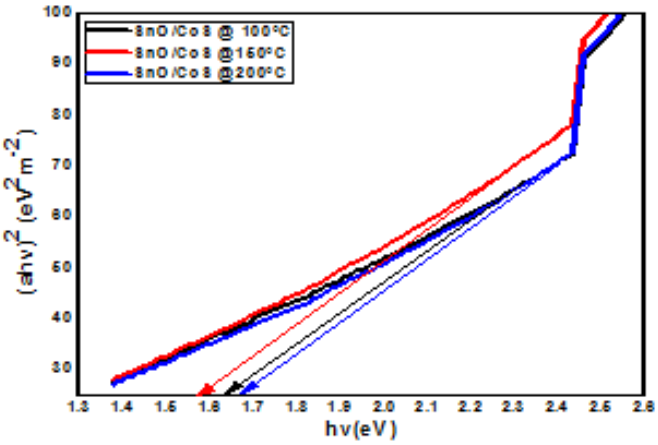

Fig.28. $(\alpha hv)^2$ (eV^2m^{-2}) Vs hv(eV) for SnO/CoS @ 100^OC, 150^OC & 200^oC.

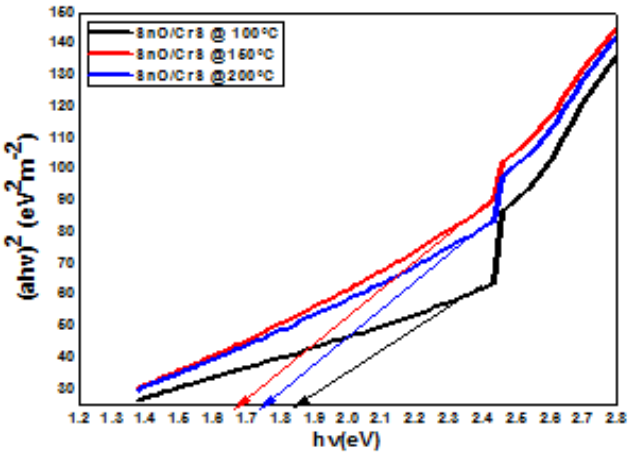

Fig. 29. $(\alpha hv)^2$ (eV^2m^{-2}) Vs hv(eV) for SnO/CrS @ 100^OC, 150^OC & 200^oC.

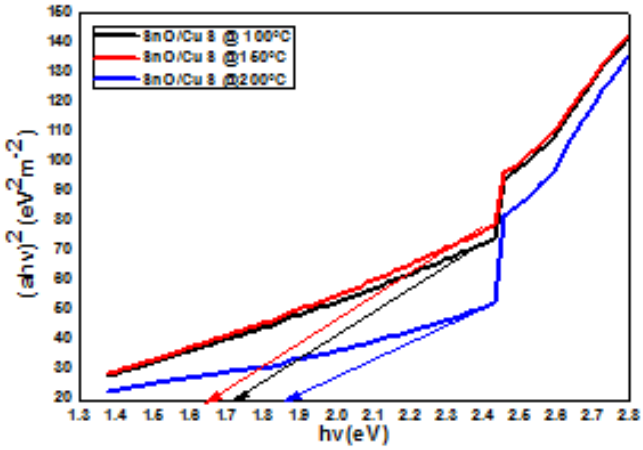

Fig. 30. $(\alpha h\nu)^2$ (eV^2m^{-2}) Vs hν(eV) for SnO/CuS @ 100°C, 150°C & 200°C.

4. Discussions

4.1. Optical and solid state properties

The optical and solid state properties such as absorbance, transmittance, reflectance, energy band gap, extinction coefficient, refractive index, real and imaginary parts of dielectric constant including optical conductivity of SnO, SnO/ZnS, SnO/CoS, SnO/CrS and SnO/CuS thin films were examined and analysed as follows:

Optical transmittance measurements of SnO thin films showed that the transparency decreased with increase in bath temperature (Fig. 1). The three layers recorded maximum transmittance in the UV region (shorter wavelength) and minimum in the infrared region (longer wavelength). This optical transmittance behaviour is averse to the report of high transmittance recorded at longer wavelength region by (Saeideh*et al.*, 2011; Igwe and Ugwu, 2010) for SnO thin films all deposited by chemical bath deposition technique. The observed optical behaviour could be attributed to the deposition conditions. The transparency generally varies from 55-98%, 31-95% and 19-93% for substrate temperatures of 100°C, 150°C and 200°C, respectively. The transmittance is generally high compared to reported values (Shadmani and Rozati, 2012). As stated earlier, the deposition conditions and other variables may be responsible for this optical behaviour. From the study of SnO/ZnS core-shell thin films, all samples exhibit high transmittance more than 90% in the ultra violet region (Fig. 2). The transparency varies from 28-95% at 100°C substrate temperature to 34-95% at 150°C substrate temperature and 48-95% at 200°C substrate temperature. When compared with the core, the core-shell did not show improvement in optical transmittance. The range of optical transmittance observed here is similar to those of Shadmani and Rozati (2012) for SnO:Zn nanostructures prepared by spray pyrolysis and Mishra *et al* (2015) for SnO_2-Al_2O_3nanocomposite synthesized via sol-gel route.In the case of SnO/CoS, SnO/CrS and SnO/CuS core-shell thin films, the transmittance spectra exhibit similar trend, maintaining a maximum in the UV region and minimum in the visible region. The peak transmittance are within the range reported elsewhere (Shadmani and Rozati, 2012; Doyan*et al*., 2019). In the Literature, the transmittance of thin films can be greatly modified by different deposition variables. Concentration dependent-optical transmission of $Mn_3O_4/Pb_{1-x}S$, $Zn_{1-x}O$, Sb_2S_3, $CuO/Pb_{1-x}S$, etc. have been reported (Augustine *et al*., 2018; Kalu*et al*., 2018; Onyishi*et al*., 2018; Augustine *et al*., 2019). Agbo and Nnabuchi (2011) reported on the transmittance of TiO_2-ZnO core-shell thin films at various annealing temperature. Many authors have investigated the optical transmission behaviour with respect to annealing temperature variations (Agbo, 2011; Agbo*et al*., 2013; Onyia and Nnabuchi, 2014; Onah*et al.*

The absorbance of SnO thin films at various bath temperatures decreases between 300-350 nmand then increases continuously up to 1000 nm(Fig. 6). This behaviour is not supported by many research works in the literature (Saeideh*et al*, 2011; Patil*et al*., 2012; Onyia and Nnabuchi,

2012). The survey of literature showed that the absorbance of thin films generally decreases with wavelength across the electromagnetic spectrum. The deposition conditions and variation of growth parameters attributed for this optical behaviour exhibited by SnO film samples deposited here. The absorbance of SnO film samples generally vary from 0.10-0.70. These range of values are within the limit stipulated by Lambert-Beer's law (online: http://www.wikilectures.eu/index-php). Our values agree with values of 0.35-0.78 by Saeideh*et al*. (2011) for SnO thin films but at variance with values 2.20-2.70 obtained by Suresh and Jiban (2015) for SnO_2 thin films all deposited by chemical bath method. The films had higher absorbance value in the infrared region as compared to other regions, which is not in agreement with higher absorbance in the UV region reported by Onyia and Nnabuchi 2015); Florian *et al*., 2019) for chemically deposited SnO thin films subjected to different annealing temperatures.

The observed optical behaviour could be attributed to the deposition conditions. SnO/ZnS biphasic thin films were found to exhibit absorbance decreases in the neighbourhood of 300-350 nm, increases from 350 nm to 600 nm and then decreases between 600-1000 nm (Fig. 5). Three major absorbance peaks of 0.35, 0.45 and 0.55 at 100^{o}C, 150^{o}C and 200^{o}C respectively were observed. The overall absorbance decreases with the coating of ZnS films on the core binary component implying zinc ion incorporation into SnO matrix. This is an indication that the optical properties of the SnO can be tuned by controlling the growth parameters of the coating materials.

The absorbance spectra of SnO/ZnS biphasic thin films also showed that it absorbs the visible region better compared to other regions unlike in the core where better absorption was observed in the infrared region. As suggested earlier, the incorporation of Zn ion into SnO film lattice which will in turn change the grain size could have accounted for the observed difference in optical behaviour. Again, there was better absorbance in thr visible region when compared to other regions whereas in the SnO, the infrared region were absorbed better compared to other regions. As explained earlier, the formation of the biphasic composites which leads to the reorientation of the cyrstal lattice and deposition conditions could have accounted for the observed optical behaviour.

This clear optical behaviour showed that we can tune the optical properties to suit a specific application by varying growth parameters. In the case of SnO/CrS biphasic thin films, the absorbance spectra followed similar trend exhibiting a maximum in the visible region and minimum in the UV region. The absorbance varies from 0.05 to 0.57 spanning the entire UV-VIS-NIR regions. The average absorbance of the biphasic composites is lower than those of the SnO. This is indication that the formation of the biphasic composites modified the absorbance spectra of the SnO. Our absorbance values are lower than those of Al-Saadi e*t al*. (2019) for SnO:Cr thin films synthesized by sol-gel method. Again, the deposition conditions and growth parameter variations could have accounted for the difference. The absorbance spectra of SnO/CuS biphasic thin films depicting peaks of 0.45, 0.42 and 0.70 for 100^{o}C, 150^{o}C and 200^{o}C layers respectively. The absorbance spectra followed similar trend with those of SnO/ZnS, SnO/CoS and SnO/CrS biphasic thin films discussed above.

The reflectance spectra of SnO thin films exhibited a similar trajectory, fluctuating between maxima and minima (Fig.11) while those of the biphasic composites exhibit similar trend as well (Fig. 12-15). The formation of the biphasic composites completely altered the reflectance spectra of binary core component. Very low reflectancewere observed for SnO/ZnS, SnO/CoS, SnO/CrS and SnO/CuSbiphasic thin films.

The high transmittance and high refractive index accounted for the observed low reflection for the biphasic thin films.

The index of refraction of a material is a physical parameter that shows the effect of the electric field component of light wave on the distribution around each of the atom in the crystal structure. Materials/atoms with high polarisable electron give rise to a high value of the index of refraction and vice versa (Agbo, 2014).The values of the index of refraction of all the film samples are not only generally low but exhibit similar trend.

The extinction coefficient (k) of the un-coated SnO thin films increased with bath temperature (Fig. 21), which differed in magnitude with those of Saturi et al. (2007) for SnO thin films deposited by radio frequency sputtering technique. Islam and Podder (2009) reported

extinction coefficient decreases with increasing substrate temperature. The deposition conditions could have accounted for the disparity in extinction coefficient behaviours. When coated with ZnS films to form SnO/ZnSbiphasic thin films, the extinction coefficient showed significant reduction in magnitude irrespective of the bath temperature (Fig. 25). In the case of SnO/CoS, SnO/CrS and SnO/CuSbiphasic thin films, the extinction coefficient exhibit similar behaviour.

The bandgap energy calculated from the absorption spectra are 2.00 eV, 2.10 eV and 2.20 eV at 100^{o}C, 150^{o}C and 200^{o}C substrate temperatures, respectively which is not exactly matching with reported bandgap energy (3.00-3.60 eV) of SnO (Patil*et al.*, 2102; Suresh and Jiban, 2015;). However, our values agree with the work of other research group in the literature (Nwodo et al., 2010). The energy band gap increases with substrate temperature indicating a blue shift. Thus the enhancement in band gap could be ascribed to enhancement of structure ordering resulting from enhancement of relative intensity of the major diffraction peak as a result of increase in substrate temperature (Ayan and Partha, 2017). The energy band gap for SnO/ZnS core-shell thin films is 1.30 eV, 1.20 eV and 1.10 eV at substrate temperatures of 100^{o}C, 150^{o}C and 200^{o}C, respectively. The energy band gap of SnO/ZnS thin films decreased with substrate temperature indicating a red shift unlike in the core-SnO where the reverse is the case. This is a clear indication that the combination of the individual binary SnO and ZnS components to form SnO/ZnS biphasic thin films modified the SnO with fascinating synergetic properties or multi functionalities offered by the composite nanostructures. The band gap decreases of SnO/ZnS biphasic thin films with substrate temperature could also be due to many body effects like the exchange energy due to electron-electron and electron-impurity interactions which occurs when the carrier density exceeds a certain value and causes narrowing (red shift) of the band gap energy (Augustine *et al*., 2018). The band gap tenability property makes SnO/ZnS biphasic thin films suitable for application in different optoelectronics devices. Our energy band gap values agree with those of Al-Saadi*et al.* (2019) while they do not agree with band gap values of 3.69-3.90 eV (Ayan and Partha, 2017), 3.75-3.9eV (Shadmani and Rozati, 2012) and 3.75-3.95 eV by Shadmani and Rozati (2012). The energy band gap values of 1.60 eV, 1.50 eV and 1.60 eV at 100^{o}C, 150^{o}C and 200^{o}C, respectively were obtained for SnO/CoS biphasic thin films while those of SnO/CrS biphasic thin films are 1.60 eV, 1.40 eV and 1.50 eV at 100^{o}C, 150^{o}C and 200^{o}C, respectively. The energy band gap values of SnO/CuS biphasic thin films vary from 1.50 eV at 100^{o}C to 1.40 eV at 150^{o}C and 1.60 eV at 200^{o}C. The energy band gap of the biphasic composite are slightly lower than those of the SnO. This is an indication that the synergetic properties of the biphasic composites affected the band gap of the SnO. In other words, the narrowing of the bandgap of baphasic thin films could be a consequence of hetrojunction which were formed with SnO film matrix. The biphasic composites shifted the fundamental absorption edge of the SnO thin films, thus providing tuning effect of the bandgap for specific application. The evaluated bandgap showed a red shift upon biphasic formation with the energy badgap decreasing from 1.30 – 1.10eV, 1.60 – 1.60 eV, 1.60 – 1.50eV, and 1.50 -1.60eV for the investigated biphasic films of SnO/ZnS, SnO/CoS, SnO/CrS and SnO/CuS respectively. Generally, the bandgap energy exhibited by these films make them ideal for use as window layer in heterojunction solar cells. CdS thin films are widely used as window layer in CIGS solar cells.

5. Conclusion

The observable breaks in the plotted graph are seen in figures 1 – 45 could be attributed to change in phase arising from the combination of SnO and TMCs coating materials during chemical bonding. It can equally be caused by quantum size effects associated with the phase transition resulting to deposition at different substrate temperatures of 100^{o}C, 150^{o}C and 200^{o}C.

The results of the research findings are stated as follows: (i) SnO/TMCs nanostructured composites configuration were successfully deposited on glass substrate using spray pyrolysis deposition technique at different substrate temperature. (i)The results of optical and solid state characterization showed that all the optical and solid state parameters varied greatly with the biphasic films of SnO/TMCs in all different substrate temperature. (ii) From the results optimal film deposition was obtained at angle of 35^{o}, height of 34.3m and substrate temperature of 200^{o}C.

(v) The evaluated band gap obtained for SnO films are 2.00 - 2.20 eV while for biphasic (SnO/TMCs) films is 1.10 - 1.60 eV. These values of bandgap make these films potential materials for window layers in CIGS solar cells or photovoltaic devices.

Acknowledgements

The authors are grateful to the Division of Material Science, Department of Industrial Physics, Ebonyi State University, Abakaliki for providing the laboratory facilities and reagents that were used for this research. We equally wish to express our profound gratitude toSheda Science and Technology Complex, Abuja, (SHESTCO) for the permission to use their laboratory for the films characterization.

References

[1] N. Abdullah, N. M. Ismail, D. M. Nuruzzaman, IOP Conf. Series: Materials Science and Engineering 319, 2018; https://doi.org/10.1088/1757-899X/319/1/012011

[2] P. E. Agbo, Journal of Chemistry and Materials Research 6(12), 68 (2014).

[3] P. E. Agbo, M. N. Nnabuchi, Chalcogenide letters 5(4), 273 (2011).

[4] P. E. Agbo, G. F. Ibeh, S. O. Okeke, J. E. Ekpe, Communications in Applied Sciences 1(1), 38 (2013).

[5] P. A. Ajibade, N. L. Botha, (2016) Synthesis, optical and structural properties of cooper sulfide nanocrystals from single molecule precursors. Department of chemistry, university of forth are, P.M.B X 1314, Alice 5700, South Africa.

[6] A. D. Ahmed, (2001) Solution growth and characterization of binary halide thin films for industrial and solar energy application, PhD Thesis, University of Nigeria, Nsukka.

[7] Alfred, Wang Wang. Y. (1994). Introduction to physics and technology of thin films, worldwide scientific publishing company, Singapore, 61.

[8] A. M. Al-Handi, U. Rinner, M. Sillanpaa, Environ. Prof. Lett. 107, 190 (2017); https://doi.org/10.1016/j.psep.2017.01.022

[9] R. M. Alluman, (1983) Sol-gel process Ulla School of Engineering and Application Science. Wikepedia. The free Encyclopedia.

[10] Al-Saadi, T.M., Hussein, B.H., Hasan, A.B. Shehab, A.A. (2019); Technologies and Materials for Renewable Energy, Environment Sustainability, 19-21 September, Athene, Greece;https://doi.org/10.1016/j.egypro.2018.11.210

[11] Anderson, Solar cell 6(2), 97 (2000); https://doi.org/10.1078/1434-4610-00010

[12] A. Antony, K.-V. Mirali, R. Manoj, M. K. Jayaraj, Materials Chemistry Physics 90(1), 106 (2005); https://doi.org/10.1016/j.matchemphys.2004.10.017

[13] S. Arthur, (1930). Practical chemistry for advanced students (1949 edition); John Murray London.

[14] Arvinte, R., Borges, J., Sousa, R.E, Munteanu, D., Baradas, N.P, Alves, E., Vaz, F &margues, L (2008) preparation and characterization of CrNxOy thin films: The effect of composition and structural features on the electrical behaviour.

[15] C. Augustine, M. N. Nnabuchi, Materials Research Express 5(1), 1 (2018).

[16] C. Augustine, R. A. Chikwenze, F. N. C. Anyaegbunam, B. J. Robert, E. P. Obot, P. N. Kalu, Global Journal of Engineeing Science and Researches 6(2), 249 (2019); https://doi.org/10.1088/2053-1591/ab1058

[17] C. Augustine, M. N. Nnabuchi, F. N. C. Anyaegbunam, A. N. Nwachukwu, Digest Journal of Nanomaterials and Biostructures 12(2), 523 (2017).

[18] M. Ayan, M. Partha, Materials Research 20(2), 430 (2017).

[19] S. G. Bailey, S. L. Castro, R. P. Raffaelle, K. K. Banger, A. F. Hepp, American Chemical

Society, 67 (2003).
[20] R.-H. Bari, S. B. Patel, International letters of Chemistry, physics and Astronomy 18, 31 (2014).
[21] Barnhart, S, Regul, T.P (1997) Occurrences, uses and properties of chromium American Chrom and Chemicals, corpus Christi, Texas, USA;https://doi.org/10.1006/rtph.1997.1132
[22] N. I. Ben, N. Kamoun, C. Guash, Applied Surface Science 234(16), 5039 (2008).
[23] H. E. Benneth, J. M. Benneth, Precession Measurement in Thin film optics, In: Hass, G and thin, R.C.(ed). Physics of Thin Film. New York. Academic press. p.56 (1967).
[24] R. Berman, Thermal, conduction in solids, claredon press oxford. 514 (2010).
[25] C. H. Bhosale, A. V. Rambale, A.V. Kotate, K. Y. Ragpure, Materials Science and Engineering 22, 67 (2005); https://doi.org/10.1016/j.mseb.2005.04.015
[26] F. J. Blalt, Physics of electronic conduction in solids, McGraw-Hill Book Company, New York, 103 (2011).
[27] S. Brown, G. Gurner, Charge and Spin-Density Waves Scientific Amaerican 270, 50 (1999); https://doi.org/10.1038/scientificamerican0494-50
[28] R. H. Bube, D. Bullis, Photoconductivity in semiconductors in photoconductivity and related phenomena, Elsevier Sc. Pub. Amsterdam, 66 (2012).
[29] J. Burgess, Metal ions in solution. New York: Ellis Horwood, 147 (1978).
[30] M. Calandra, I. I. Mazin, F. Maurim, Phys. Rev B: Condens Matter mater. Phys. 2009, 80 (2009); https://doi.org/10.1103/PhysRevB.80.241108
[31] F. M. Ciro, A. A. Migreal, G. H. Manuel, Spray Pyrolysis techniques High-K Dietetic films and luminescent materials. A review Development Ode Fisica,(INVESTAN) 615, 756 (2018).
[32] R. A. Chikwenze, M. N. Nnabuchi, Chalcogenide Letters 7(5), 401 (2010).
[33] K. L. Choptra, R. C. Keninthia, D. K. Pandy, A. P. Thakoor, (1991) Physics of Thin films PP 125 Academic Press, London.
[34] K. L. Chorpa, S. R. Das, Thin film solar cells. London: Plenum press, 4,8,13,59,72,96,102 (1983).
[35] L. P. Colletti, D. Teklay, J. L. Stickney, Journal of Electroanalytical Chemistry 369, 145 (1994); https://doi.org/10.1016/0022-0728(94)87092-6
[36] V. L. Colvin, M. C. Seltap, A. P. Alivisator, Nature 370, 354 (1994); https://doi.org/10.1038/370354a0
[37] U. C. Davis, (2019) General Properties and Reactions of oxygen family (the chalcogens oxygen Group VIA) friends. Chemistry Libre Texts 2019 library University of California.
[38] C. Deshpandey, R. F. Bundshah Journal of thin solid films 163, 131 (1988); https://doi.org/10.1016/0040-6090(88)90418-X
[39] Doyan, A., Susilawati, Hakin, S., Muliyadi, L., Tanfik, M. and Nazarudin (2019). Journal of Physics: Conference Series, https://doi.org/10.1088/1742-6596/1397/1/012005
[40] Egon, W. and Amold, F.H. (2001). Inorganic chemistry, Elsevier ISBN 0-12-352651-5.
[41] A. J. Ekpunobi, N. A. Okeke, Journal of Optoelectronic and Biomedical Materials 3(3), 69 (2011).
[42] Ahmed El Hiti, M. A. El-Shabasy, Journal of Materials Science letters S, 329 (1989); https://doi.org/10.1007/BF00725514
[43] F. C. Eze, C. E. Okeke, Journal of Material Chemistry and Physics 47, 31 (1997); https://doi.org/10.1016/S0254-0584(97)80024-7
[44] F. I. Ezema, (2000). Solution growth and characterization of binary and ternary thin halide and chalcogenide films for industrial and solar energy applications- PhD Thesis University of Nigeria, Nsukka.
[45] N. Fathy, R. Kobayashi, M. Ichimura, Materials Science and Engineering B 107(3), 271 (2004); https://doi.org/10.1016/j.mseb.2003.11.021
[46] P. Goli, J. Kham D. Wickramaratne, R. K. Lake, A. A. Balandin, Nanoletters 12, 5941 (2012); https://doi.org/10.1021/nl303365x

[47] G. Goncales, A. Pimental, A. Fortnato, E. Martins, R. Quiroz, R. F. Burchy, R. M. Faria, Journal of Non-Crystal Solid, 1444 (2006); https://doi.org/10.1016/j.jnoncrysol.2006.02.021

[48] G. Huang, T. Chen, Z. Wang, K. Chnag W. Chen, J. power sources 2, 122 (2013); https://doi.org/10.1016/j.jpowsour.2013.01.093

[49] H. U. Igwe, E. I. Ugwu, Advances in Applied Science Research 1(3), 240 (2010).

[50] B. Ismail, S. Mushtaq, A. Khan, Chalcogenide Letters 11(1), 37 (2014).

[51] P. N. Kalu, D. U. Onah, P. E. Agbo, C. Augustine, R. A. Chikwenze, Middle-East Journal of Scientific Resrach 26(5), 543 (2018).

[52] P. N. Kalu, D. U. Onah, P. E. Agbo, C. Augustine, R. A. Chikwenze, F. N. C. Anyaegbunam, C.O. Dike, Journal of Ovonic Research 14, 293 (2018).

[53] R. Kamruzzaman, J. Podder, (2011) Synthesis characterization of the As deposited Cd, xpbxs thin films prepared by spray pyrolysis technique. Journal Pletades Publishing ISSN 1063-7826, Semi-conductors.

[54] U. I. Kasim, A. Umar, I. Adamu, I. K. Mohammed, E. U. Uno, Influence of dye Ph on photoelectric properties of dye sensitized solar cells using natural dye extracted from red bougainvillea glabra flower, 1st African International Conference/Workshop on Applications of Nanotechnology to Energy, Health and Environment, UNN, March 23-29, 2014, 158 (2014).

[55] Kinsley EivelUkoba (2018) Study of Optoelectronic properties of nanostructured Tio2/N:O Heterojunction solar cells. Proceeding of the world congress on Engineering and Computer Science 2018, Vol. I WCECS.

[56] Lee, D.L (1996). Concise Inorganic Chemistry Gopsons Paper Ltd London, 680-796.

[57] M. Liao, C. Erhu, J. David, Y. Cheng, Nature International Journal of Science 504(7478), 107 (2013); https://doi.org/10.1038/nature12822

[58] Liping W., Yujie S., and Xiaodong X. (2013). Structure and optical properties of Cu-doped ZnS nanoparticles formed in chitosan/sodium alginate multilayer films. Online library wiley.com.

[58] I. D. Lokhande, V. S. Yermune, S. H. Pawar, Materials Chemistry and Physics 20(3), 283 (2016); https://doi.org/10.1016/0254-0584(88)90068-5

[59] O. Lopez Sanchez, D. Lembke, M. Kayci, A. Radenovic, A. Kis, Nature nanotechnology 8, 497 (2013); https://doi.org/10.1038/nnano.2013.100

[60] N. A. Mahwood, (2013) Optical materials, willey Inc. New York, 112

[61] B. G. Manoj, A. Anandraup Git Tewodors, G. Huizhnag, V. B. Ankush, P. Dong-Linag, RadekZborit, V. Rejender, chalcgenide letters 3(2), 101 (2015).

[62] D. Maring, M. Cristain, Adriana Smarandache, P. Gabriel, Beilstein J. Nanotechnol 10, 9 (2019); https://doi.org/10.3762/bjnano.10.2